

JPET #241661

Synergistic antiproliferative activity of the RAD51 inhibitor IBR2 with inhibitors of receptor tyrosine kinases and microtubule protein

Peter J. Ferguson, Mark D. Vincent, and James Koropatnick

London Regional Cancer Program and Lawson Health Research Institute, London, Ontario, Canada (P.J.F., M.D.V., J.K.); Departments of Microbiology and Immunology (J.K.), Pathology (J.K.), Physiology & Pharmacology (J.K.), and Oncology (P.J.F., M.D.V., J.K.), University of Western Ontario, London, Ontario, Canada

JPET #241661

Running title: Synergy between RAD51 inhibitor IBR2 and chemotherapy drugs

Corresponding author:

Peter Ferguson

Cancer Research Laboratory Program - London Regional Cancer Program

London Health Sciences Centre, 790 Commissioners Road East

London, Ontario, Canada N6A 4L6

Phone: 519-685-8500 Ext 53602

FAX: 519-685-8616

peter.ferguson@uwo.ca

Number of text pages: 32

Tables: 0

Figures: 7

Number of References: 31

Number of words in abstract: 244

Number of words in Introduction: 526

Number of words in Discussion: 1342

Abbreviations: AML, acute myeloid leukemia; CML, chronic myeloid leukemia; EGFR, epidermal growth factor receptor; HNSCC, head and neck squamous cell carcinoma; HR, homologous recombination; Hsp90, heat shock protein 90; IC₅₀, concentration of drug that inhibited proliferation by 50%; LFA2K, Lipofectamine 2000©; MDR, multidrug resistant; NSCLC, non-small-cell lung cancer; PARP, poly(ADP-ribose) polymerase; PDGFR,

JPET #241661

platelet-derived growth factor receptor; Pgp, P-glycoprotein; SCLC, small cell lung cancer.

Recommended section assignment: Drug Discovery and Translational Medicine

Abstract

Although cancer cell genetic instability contributes to characteristics that mediate tumorigenicity, it also contributes to the tumor-selective toxicity of some chemotherapy drugs. This “synthetic lethality” can be enhanced by inhibitors of DNA repair. To exploit this potential “Achilles heel”, we tested the ability of a RAD51 inhibitor to potentiate the cytotoxicity of chemotherapy drugs. 2-(benzylsulfonyl)-1-(1H-indol-3-yl)-1,2-dihydroisoquinoline (IBR2) inhibits RAD51-mediated DNA double-strand break repair but also enhances cytotoxicity of the Bcr-Abl inhibitor imatinib. The potential for synergy between IBR2 and more drugs was examined *in vitro* across a spectrum of cancer cell lines from various tissues. Cells were exposed to IBR2 simultaneously with inhibitors of receptor tyrosine kinases, DNA-damaging agents, or microtubule disruptors. IBR2, at concentrations that inhibited proliferation between 0% and 75%, enhanced toxicity by up to 80% of imatinib, regorafenib (targets RAF, kit), EGFR inhibitors erlotinib, gefitinib, afatinib and osimertinib, and vincristine, an inhibitor of microtubule function. However, IBR2 antagonized the action of olaparib, cisplatin, melphalan, and irinotecan. A vincristine-resistant squamous cell line was not cross-resistant to imatinib, but IBR2 and another RAD51 inhibitor (B02) enhanced imatinib toxicity in this cell line, its HN-5a parent, and the colon cancer line HT-29 by up to 60% and much better than verapamil, a P-glycoprotein inhibitor ($P < 0.05$). Given the disparate agents the functions of which are enhanced by IBR2, the mechanisms of enhancement may be multimodal. Whether RAD51 is common to these mechanisms remains to be elucidated, but it provides the potential for selectivity to tumor cells.

Introduction

The success of anticancer chemotherapy is often limited by the development of drug resistance by tumors, a phenomenon that evolves spontaneously due to the inherent genetic instability of cancer cells. This same feature renders cancer cells more sensitive than normal cells to many kinds of cytotoxic insult and contributes to the often limited selectivity of anticancer agents for tumor cells. However, some cancer cells have significant deficits in specific guardians of genomic maintenance, contributing to even greater sensitivity to agents that target particular enzymes or biochemical pathways. This specific hypersensitivity is referred to as synthetic lethality and has been exploited to treat tumors that develop and/or progress as a result of specific lesions promoting genetic instability. For example, breast cancers that develop due to the absence of functional BRCA1 or BRCA2, important in HR-dependent DNA repair, are more sensitive to treatment with inhibitors of other DNA repair pathways, namely inhibitors of PARP (Bryant *et al.*, 2005; Farmer *et al.*, 2005).

Since tumors with inherent, pre-existing molecular alterations that provide synthetic lethal opportunity comprise only a small minority of cancer cases, induction of synthetic lethality in tumors without such pre-existing alterations would expand opportunities for chemotherapy success. Induced synthetic lethality would create selective sensitivity to specific drugs, allow use of lower doses, and spare toxicity to normal tissues. We have demonstrated induction of synthetic lethality by decreasing the levels of BRCA2 in cultured tumor cell lines, enhancing their sensitivity to inhibitors of PARP and other biochemical targets (Ferguson *et al.*, 2013; Rytelewski *et al.*, 2013; Rytelewski *et al.*, 2016). More recently, this form of induction includes

down-regulation of RAD51 to sensitize a variety of cancer cell lines to a plethora of anticancer drugs (Ferguson *et al.*, 2016). RAD51 is an essential protein for HR-dependent DNA repair (Godin *et al.*, 2016).

It was therefore appropriate to determine the ability of a small molecule inhibitor of a DNA damage repair protein to enhance sensitivity to anticancer agents. Although there are currently no commercially available inhibitors of BRCA1 or 2, several inhibitors of RAD51 have been reported. IBR2 [2-(benzylsulfonyl)-1-(1H-indol-3-yl)-1,2-dihydroisoquinoline] was designed to specifically bind to and inhibit RAD51 (Lee W-H, *et al.*, 2009). IBR2 downregulates the protein level and repair activity of RAD51, presumably inducing apoptosis through development of toxic double-strand DNA lesions leading to *in vivo* tumor growth inhibition (Zhu *et al.*, 2013). IBR2 also enhanced sensitivity of K562 CML cells to imatinib (Gleevec®) (Zhu *et al.*, 2013), an inhibitor of Bcr-Abl that also inhibits c-kit and PDGFR. The ability of IBR2 to enhance imatinib and multiple other anticancer agents was examined across a range of human tumor cell lines, since their dependence on various oncogenic drivers could lend evidence to the mechanism of the enhancement. IBR2 was tested in combination with regorafenib, which inhibits multiple molecules, including all of those inhibited by imatinib. Other drugs tested included inhibitors of EGFR and microtubule function, and DNA-damaging agents. The findings indicate that IBR2 sensitizes cells to numerous agents. It is unclear whether RAD51 is directly involved in the enhancement of antiproliferative activity of these agents by IBR2. Some of the findings suggest that other targets for IBR2 may be involved.

Materials and Methods

Cells: The human HNSCC cell line HN-5a was established at The University of Western Ontario from the gingival tumor of a patient not previously treated with chemotherapy or radiation (Lapointe *et al.*, 1992). The MDR, Pgp-expressing cell line HN-5a/V15e was established as previously described (Ferguson *et al.*, 2009). The SCLC cell line H69 was provided by Dr. Susan Cole, Queen's University, Kingston, Canada (Slovak *et al.*, 1993). All other cell lines were obtained from American Type Culture Collection. A clonal line of NSCLC cell line A549 (A549b) was propagated from a single cell.

Chemicals: IBR2 was obtained from Drs. Jiewen Zhu and Wen-Hwa Lee, University of California - Irvine (Lee *et al.*, 2009). Cisplatin was obtained from Mayne Pharma (Montreal, Canada). Olaparib, imatinib, osimertinib, and afatinib were purchased from Cedarlane Labs (Burlington, Canada). siRNA targeting RAD51 mRNA (ON-TARGETplus), BRCA2 mRNA (Rytelewski *et al.*, 2013) and non-targeting sc-RNA #2 were obtained from Dharmacon/Thermo Fisher Scientific (Lafayette, CO, USA). Anti-RAD51 siRNA 51-a targets mRNA sequence 5'-UAUCAUCGCCCAUGCAUCA-3' [coding region, bases 1169-1187 (NM_002875.4)]. All other compounds were obtained from Sigma-Aldrich (Oakville, Canada).

Other materials: Fetal bovine serum and LFA2K were purchased from Invitrogen/ThermoFisher (Unionville, Canada). Cell culture plastic-ware was obtained from Invitrogen/Fisher Scientific and VWR (Mississauga, Canada). Cell culture media and chemicals were obtained from commercial sources.

Proliferation assays: Cells were maintained in minimum essential medium alpha plus 10% fetal

JPET #241661

bovine serum and penicillin (50 units/mL)/streptomycin (50 mg/L) (growth medium). Cultures were incubated in a humidified atmosphere of 5% CO₂ at 37°C. Rapidly proliferating cells were used to establish cultures of experimental cells, which were allowed to plate overnight in 96-well plates or 25-cm² flasks prior to manipulation.

Exposure to chemotherapy drug plus IBR2, verapamil, or B02: Cells were grown in 96-well plates and treated with simultaneous exposure to the drugs at the concentrations indicated. The relative cell density was determined after 4 days by viability staining (AlamarBlue® or neutral red). The relative density of cells treated with both agents was normalized to the density observed for the respectively treated “second agent” control (IBR2, verapamil, or B02). The concentration of drug that inhibited proliferation by 50% (IC₅₀ value) was interpolated from plotted data. The change in the IC₅₀ value of a chemotherapy drug caused by the presence of the second agent was determined as a percent of the IC₅₀ of the first drug alone (Suppl. Fig.1). Enhancement of cytotoxicity is indicated by a decrease in the IC₅₀ value. This methodology, previously reported (Ferguson *et al.*, 2009; Blake *et al.*, 2017), provides a quantitative, concentration-dependent representation of the magnitude of the drug interaction.

Antisense treatment: Cells were grown in 25-cm² flasks, and allowed to plate overnight. siRNA was introduced into cells with the use of LFA2K, mixed at a ratio of 1.25 µg/ml per 10 nM siRNA in serum-free medium. The mixture was prepared at 5x the final concentration to which cells were exposed, so that 0.5 ml was added to 2 ml of medium in which cells were plated. After incubating at room temperature for 20 min, according to manufacturer's instructions, the nucleic acids were added to the cell medium, and incubated (37°C) on the cells for 4 hours, after which a

JPET #241661

second volume of medium was added. Cells were then incubated for 20 h. Following this incubation, the siRNA-containing medium was replaced with drug-free medium. If the cells were to be exposed to a drug, for the purposes of determining whether inhibitory activity was enhanced by the antisense pretreatment, the drug was added at this time. At this point, replicate flasks from the antisense treatment were used to enumerate cell content, as this varied among treatments over the initial 24-h exposure. This was done so that the effect of the second treatment can be ascertained based on the cell population that was present at the time of initiation of exposure. Exposure to the second drug was initiated by addition of 0.2-volume of a drug preparation, at 6x final concentration in growth medium, to the fresh, drug-free medium on the cells (1 ml of drug into 5 ml of medium). Following a further 4-day incubation, the proliferation of the treated cells (fold-increase in cell number) was calculated as a percentage of that of control cells. Cell numbers were enumerated on an electronic particle counter (Coulter Z1, Beckman Coulter, Mississauga, Canada).

Flow cytometry. A549b cells were incubated in IBR2 for 24 h, followed by harvesting with trypsin, washing with PBS, and fixing in 70% ethanol. Fixed cells were stained with propidium iodide and analyzed with a flow cytometer (10,000 events) (BD LSR II, BD Biosciences, Mississauga, Canada) in the London Regional Flow Cytometry Facility, Robarts Research Institute, Western University, London, Canada. The percent of cells in each of G1, S, and G2/M phases was determined using the curve-fitting program FlowJo (FlowJo LLC, Ashland, OR).

Statistical evaluation: Differences between data sets were compared using a 2-tailed Student's t-test. Significance levels were set a priori at $P < 0.05$.

Results

To determine if IBR2 could have a broader usage to enhance the antitumor effect of chemotherapy drugs, the combination of IBR2 plus a range of drugs was tested against a panel of cancer cell lines derived from tissues that included lung, head and neck, gastric (stomach), breast, colon, prostate, and hematopoietic cells (AML and CML). The cell lines expressed a range of different oncogenic drivers, including chimeric Bcr-Abl (K562), mutations of k-RAS (A549b, AGS, HCT-15) or b-Raf (HT-29), and mutant (Kasumi-1) or overexpressed c-Kit (H69), although some cell lines were of less descript etiology (Hs746T, N87, MCF-7, DU145) (information from American Type Culture Collection website)¹. A virally transformed, human embryonic kidney cell line (HEK293) was also included in several of the analyses. Sensitivity to IBR2 was very similar across all of the cell lines studied, in which the IC₅₀ values ranged between 15 and 25 μ M (Fig. 1, Suppl. Fig. 1). Sensitivity to imatinib and regorafenib ranged more broadly, and Kasumi-1, which expresses mutant c-Kit, was highly sensitive to both of these. In A549b cells, IBR2, at concentrations that inhibited proliferation by greater than 50%, induced a significant accumulation of cells in G1, at the expense of a decrease of population in S and G2/M (Suppl. Fig. 2). For the drug-combination studies described below, IBR2 was used at concentrations that inhibited proliferation by up to 75%.

When IBR2 was combined with imatinib, as previously demonstrated in K562 cells (Zhu *et al.*, 2013), the antiproliferative activity of imatinib was enhanced by 40-60% in many of the cell lines (Fig. 2). Panel A in Fig. 2 is an example of the shift of the dose-response curves to lower imatinib concentrations in the presence of IBR2, in a concentration-dependent manner

JPET #241661

(AGS stomach cancer cell line in this example). The amount by which the curves were shifted was quantified for each curve in individual experiments, as a function of the change in IC_{50} value (demonstrated in Suppl. Fig. 3). Other representative experiments, demonstrating the leftward shift in the dose-response curve, are presented in Suppl. Figs. 4-6. It is noteworthy that not only were the curves shifted to the left, but in most instances there were concentrations of IBR2 and drug that completely inhibited proliferation; as single agents, these concentrations inhibited proliferation by only 20-60%, and often only 20-40% (Suppl. Figs. 1, 4-6). Although such extensive inhibition was observed in each experiment, it is cumbersome to report for the large number of combinations of drug concentrations. Therefore, the shift in IC_{50} value was chosen for analysis of the effects demonstrated herein because it is readily quantifiable and is reproducible between experiments. The amount of change in IC_{50} , calculated as a percent of that IC_{50} value, was determined for a variety of concentrations of IBR2 against 12 of the cell lines (Fig. 2, Panels B - D). IBR2 was not as effective at enhancing imatinib cytotoxicity in some cell lines as it was in others, indicating that there was some cell-specificity to the degree of enhancement.

To determine whether IBR2 could also enhance cytotoxicity of other chemotherapy drugs, it was tested in combination with agents that have a variety of biochemical targets. Regorafenib targets RAF, kit, and a variety of growth factor and angiogenic receptor kinases. IBR2 enhanced the antiproliferative activity of regorafenib by up to 60 - 80% in all of the cell lines tested except for Kasumi-1 (Suppl. Fig. 5, Fig. 3), which was already very sensitive to regorafenib (and reflective of a similar situation with response to imatinib in this cell line).

EGFR was chosen as a different biochemical target against which to determine whether

JPET #241661

its inhibitors could be enhanced by IBR2. For this assay, 3 NSCLC cell lines were used, as this tumor type is commonly treated with EGFR inhibitors clinically, but usually relapses with resistance to the drug. A variety of responses was observed when IBR2 was combined with different EGFR inhibitors (Suppl. Fig. 6, Fig. 4). Although IBR2 enhanced gefitinib toxicity against all 3 cell lines, there was no interaction with afatinib in A549b cells or erlotinib in H1975 cells, and there was even antagonism between IBR2 and erlotinib against A549b cells. Erlotinib tends to cause a plateau in proliferation at approximately 50% at concentrations of 10 μ M and above (tested to 50 μ M), which is indicative of a cytostatic effect. This may account for the apparent antagonism when combined with IBR2. Against HEK293, although there was a small amount of enhancement of gefitinib and osimertinib by lower concentrations of IBR2, there was strong antagonism at higher concentrations that were synergistic against the cancer cell lines.

Based on limited information that imatinib may be a substrate for a multidrug transport protein (Radujkovic *et al.*, 2005), there existed the possibility that IBR2 was acting to enhance drug activity by inhibiting a drug exporter, such as Pgp, thus increasing the intracellular drug accumulation. Therefore, the effect of combining IBR2 with imatinib was compared with the Pgp inhibitor verapamil against 4 different cell lines, including one cell line that overexpresses Pgp and is 3-fold resistant to vincristine (HN-5a/V15e) (Fig. 5) (Ferguson *et al.*, 2009). As another comparison with these combinations, a second RAD51 inhibitor, B02 (Huang *et al.*, 2012), was tested. Against all 4 cell lines tested, including HN-5a/V15e, IBR2 and B02 were more effective than verapamil at enhancing the antiproliferative activity of imatinib. It is also noteworthy that HN-5a/V15e is not cross-resistant to imatinib (Fig. 1).

JPET #241661

In combination with vincristine against these same 4 cell lines (Fig. 6), IBR2, B02 and verapamil exhibited similar enhancement at most concentrations with the following exceptions: in HT-29 cells, IBR2 was not as effective as B02 and verapamil at concentrations of 5 μ M and higher, but IBR2 and B02 were more effective than verapamil at 2 μ M and lower; as expected in vincristine-resistant HN-5a/V15e (since verapamil is a classic inhibitor of Pgp), verapamil enhanced vincristine cytotoxicity better than IBR2 and B02, especially at lower concentrations.

Antisense knockdown of BRCA2 enhanced the antiproliferative activity of the PARP inhibitor olaparib by 50% (Rytelewski *et al.*, 2016; Suppl. Fig. 7A), and, similarly, antisense siRNA against RAD51 also sensitized cell lines to inhibition by olaparib (Fig. 7A and C). In contrast: (1) knockdown of BRCA2 had no effect on cytotoxicity of IBR2 (Suppl. Fig. 7B); (2) the combination of IBR2 and olaparib was antagonistic (Fig. 7B) or additive only (Suppl. Fig. 8), indicative of a possible interaction that is required between PARP and RAD51 in order for olaparib to incur DNA damage; and (3) anti-RAD51 siRNA, at concentrations that greatly enhanced olaparib toxicity, only slightly enhanced toxicity of drugs with which IBR2 was synergistic, and in some combinations was antagonistic (Fig. 7D).

The enhancement of drug toxicity by IBR2 demonstrated specificity to certain drug classes, and did not include those that directly damage DNA. IBR2 was not able to enhance cytotoxicity of paclitaxel, irinotecan, melphalan, or cisplatin (Suppl. Fig. 9).

Discussion

IBR2 is among several recently developed RAD51 inhibitors (Zhu *et al.*, 2013; Balbous *et al.*, 2016; Lv *et al.*, 2016; Huang *et al.*, 2012), one of which enhances cell sensitivity to x-irradiation (Lv *et al.*, 2016). Another, B02, when combined with a PARP inhibitor, synergistically enhances the DNA-damaging agent methylmethane sulfonate (Huang *et al.*, 2012). B02 was chosen for comparison purposes in the current study to help demonstrate whether the synergistic interactions between IBR2 and chemotherapy drugs could be attributable to a direct effect on RAD51.

IBR2 enhanced cytotoxicity of anticancer agents having a variety of biochemical targets, including: imatinib (targets Bcr-Abl, c-kit, PDGFR); regorafenib (RAF, kit, various growth factor and angiogenic receptor kinases); inhibitors of EGFR (erlotinib, gefitinib, afatinib, osimertinib); and vincristine (microtubules). Although IC₅₀ values were decreased by up to 80%, inhibition of proliferation was 95-100% at many drug concentrations that alone were not substantially inhibitory (e.g., see Suppl. Figs. 4-6). Therefore, IBR2-drug combinations have the potential to fully inhibit tumor growth *in vivo* at doses that are minimally inhibitory on their own. For purposes of data interpretation, the choices of “drug” and “enhancing agent” (or “second agent”) are arbitrary, and the numbers could be used to indicate that imatinib, for example, enhanced IBR2 cytotoxicity. Because the concentrations of IBR2 used in these combinations inhibited proliferation between 0% and 75% as a single agent, there were instances in which the synergy between the 2 agents could be a result of enhancement of IBR2 toxicity (discussed below). However, in most combinations, IBR2, verapamil, and B02 were considered as the

JPET #241661

enhancing agent for two reasons: (1) they were tested in combination with many different chemotherapy drugs and were designated as the second agent for purposes of clarity and to facilitate comparisons between experiments; and (2) synergy was observed in many instances when the second agent was used at non-toxic concentrations.

The enhancement of cytotoxicity by IBR2 was not a broad-spectrum, non-specific effect. IBR2 sometimes had no effect on the drug, in which case the change in IC_{50} value induced by IBR2 was zero. In some instances IBR2 interfered with or antagonized the toxicity of the drug, in which case the change in IC_{50} value was positive (for examples see Suppl. Fig. 9). Also, IBR2 did not enhance cytotoxicity of imatinib or regorafenib in Kasumi-1 cells, which are inherently sensitive to these agents.

The differences in the IBR2/drug interactions between the different drugs used indicate mechanistic specificity of the interaction, although at this point it is not possible to distinguish the basis of the selectivity. The above results and other evidence suggest that IBR2 may have several modes of action that confer its ability to enhance cytotoxicity of a variety of anticancer agents:

(1) IBR2 enhanced cytotoxicity of drugs with disparate biochemical targets, including signal transduction proteins belonging to different pathways, and the microtubule disruptor vincristine (but not paclitaxel, except in the MDR cell line). RAD51 is not linked directly with any of these functions.

(2) In K562 cells (mutant c-Kit, Bcr-Abl expression), IBR2 enhanced regorafenib, which targets c-Kit. c-Kit and RAD51 are both client proteins of Hsp90, as are Bcr-Abl, Akt, and BRCA1

(Smyth *et al.*, 2012; Suhane *et al.*, 2015; Noguchi *et al.*, 2006; Jiang *et al.*, 2017). In Kasumi-1 cells (normal Abl, mutant c-Kit), which are hypersensitive to imatinib and regorafenib (Fig. 1; Beghini *et al.*, 2005), IBR2 conferred minimal enhancement.

(3) Given that IBR2 inhibits the protein expression and activity of an essential DNA repair protein, it was expected that IBR2 would enhance cytotoxicity of drugs that directly damage DNA (melphalan, cisplatin, irinotecan). The fact that this was not the case indicates that a secondary mechanism of repair may compensate for inhibition of RAD51 (Wiegmans *et al.*, 2016), but this mechanism does not compensate for the effects that enhance toxicity of non-DNA-damaging agents.

(4) Since IBR2 enhanced vincristine cytotoxicity, a possible interaction with Pgp was investigated. The Pgp-overexpressing, MDR cell line HN-5a/V15e was not cross-resistant to imatinib nor IBR2 (Fig. 1), suggesting that Pgp does not modulate imatinib activity in this cell line. [In contrast, imatinib has been reported to be a Pgp substrate in other cells (Radujkovic *et al.*, 2005)]. IBR2 enhanced imatinib toxicity in HN-5a/V15e, its parent line HN-5a, and HT-29 by up to 60%, much better than verapamil (up to 40% at similar concentrations, $P < 0.05$). IBR2 enhanced vincristine toxicity in these 3 cell lines to a degree similar to verapamil, decreasing the IC_{50} by up to 90%. Therefore, there is no conclusive evidence that IBR2 interacts with Pgp to enhance drug cytotoxicity.

(5) Another RAD51 inhibitor, B02, displayed similar enhancement of imatinib and vincristine as IBR2 (Huang *et al.*, 2012). Although this molecule may likewise not necessarily be specific for RAD51, it suggests an overlapping mechanism of enhancement of drug toxicity by 2 compounds

that were designed as specific inhibitors of RAD51.

(6) The PPAR γ inhibitor T007 decreases α and β tubulin proteins in some cancer cell lines and also appears to inhibit RAD51 (An *et al.*, 2016). This suggests that inhibitors of DNA repair, possibly including a RAD51 inhibitor, may influence the activity of microtubules, and may contribute to the sensitization of cell lines to vincristine, as reported herein.

(7) Modulators of protein turnover decrease levels of RAD51 as well as various proteins involved in signal transduction and DNA repair (Segawa *et al.*, 2014; Ko *et al.*, 2012; Smyth *et al.*, 2012).

(8) Bcr-Abl upregulates RAD51 (Slupianek *et al.*, 2001, Suhane *et al.*, 2015; Noguchi *et al.*, 2006; Jiang *et al.*, 2017). Therefore, in a cell line such as K562 which is dependent on Bcr-Abl as its oncogenic driver, the Bcr-Abl inhibitor imatinib could potentially cause a decrease in RAD51, increasing sensitivity to IBR2.

(9) IBR2 generally enhanced activity of inhibitors of EGFR. The exception was erlotinib, for which the interaction ranged from synergistic to nil to antagonistic.

(10) Akt and EGFR are both suggested to regulate the level of RAD51 (Ko *et al.*, 2016; Zhong *et al.*, 2016). Therefore, an inhibitor of EGFR could potentially decrease the level of RAD51, making the cell more sensitive to a RAD51 inhibitor.

(11) For the following reasons, Hsp90 was considered as a possible secondary target for IBR2: (i) inhibition of Hsp90 (A549, H1975) or its yeast ortholog Hsp82 results in decreased RAD51 (degradation by proteosomes) and inhibits DNA repair (Suhane *et al.*, 2015; Segawa *et al.*, 2014; Ko *et al.*, 2012); (ii) the Hsp90 inhibitor 17-AAG down-regulated Bcr-Abl protein level in CML

JPET #241661

cells, and acted synergistically with imatinib to kill Bcr-Abl-overexpressing CML cells (Radujkovic *et al.*, 2005); (iii) Hsp90 is a chaperone for EGFR and Bcr-Abl (Jhaveri *et al.*, 2014); and (iv) inhibition of Hsp90 sensitizes human lung cancer cell lines to treatment with inhibitors of EGFR (Courtin *et al.*, 2016). Therefore, the Hsp90 inhibitor 17-AAG was tested in combination with several drugs against various cell lines (Suppl. Figs. 10-13). 17-AAG, which is cytotoxic in the nanomolar range (Suppl. Fig. 10), was not synergistic with imatinib, osimertinib, or vincristine, but showed good synergy with gefitinib at most concentrations, except against HEK293 (Suppl. Figs. 12-13). The minimal synergy between 17-AAG and a range of drugs tends to preclude Hsp90 as a secondary target of IBR2.

(12) The inability of antisense against RAD51 to recapitulate the synergy between IBR2 and 4 chemotherapy drugs suggests that IBR2 may have secondary targets and/or requires the presence of RAD51 to create an inhibitory entity.

Notwithstanding these observations, it remains possible that interaction of IBR2 with RAD51 or another, non-specific target has a common node of interactions among the various targets of the drugs assayed herein. IBR2 was most effective in sensitizing human cancer cell lines to treatment with imatinib, regorafenib, EGFR inhibitors (including erlotinib, gefitinib, afatinib, and osimertinib), and vincristine. It may have less potential for useful combination with olaparib, melphalan, cisplatin, paclitaxel (in non-Pgp-overexpressing tumors), or irinotecan. The potential for IBR2 to induce synthetic lethality and increase selectivity of anticancer treatment, sparing normal tissues and improving the overall success of numerous treatments, is worthwhile to investigate in animal models.

JPET #241661

Acknowledgements

Portions of this work were presented in abstract form: Ferguson PJ, Vincent MD, and Koropatnick J. Synergistic anticancer activity of the targeted drugs imatinib, regorafenib, and gefitinib with the RAD51 inhibitor IBR2. Proceedings of 28th EORTC-NCI-AACR Symposium on Molecular Targets and Cancer Therapeutics, Munich, Germany. Abst. 368, 2016.

The authors would like to thank Mrs. Ronak Zareardalan, Dr. Saman Maleki, and Dr. Kristin Chadwick for technical assistance with cytotoxicity assays (RZ) and flow cytometry (SM, KC).

This work is dedicated to the memory of Mrs. Mary Ferguson.

Authorship Contributions

Participated in research design: Ferguson, Koropatnick and Vincent.

Conducted experiments: Ferguson.

Performed data analysis: Ferguson.

Wrote or contributed to the writing of the manuscript: Ferguson, Koropatnick and Vincent.

References

An Z, Yu JR, and Park WY (2016) T0070907 inhibits repair of radiation-induced DNA damage by targeting RAD51. *Toxicol In Vitro* 37: 1-8. doi: 10.1016/j.tiv.2016.08.009; corrigendum: doi: 10.1016/j.tiv.2016.11.013

Balbous A, Cortes U, Guilloteau K, Rivet P, Pinel B, Duchesne M, Godet J, Boissonnade O, Wager M, Bensadoun RJ, Chomel JC, and Karayan-Tapon L (2016) A radiosensitizing effect of RAD51 inhibition in glioblastoma stem-like cells. *BMC Cancer* 16: 604. doi: 10.1186/s12885-016-2647-9.

Beghini A, Bellini M, Magnani I, Colapietro P, Cairoli R, Morra E, and Larizza L (2005) STI 571 inhibition effect on KITAsn822Lys-mediated signal transduction cascade. *Exp Hematol* 33: 682-688.

Blake A, Dragan M, Tirona RG, Hardy DB, Brackstone M, Tuck AB, Babwah AV, Bhattacharya M (2017) G protein-coupled KISS1 receptor is overexpressed in triple negative breast cancer and promotes drug resistance. *Sci Rep* 7: 46525; doi: 10.1038/srep46525

Bryant HE, Schultz N, Thomas HD, Parker KM, Flower D, Lopez E, Kyle S, Meuth M, Curtin NJ, and Helleday T (2005) Specific killing of BRCA2-deficient tumours with inhibitors of poly(ADP-ribose) polymerase. *Nature* 434: 913-917.

Courtin A, Smyth T, Hearn K, Saini HK, Thompson NT, Lyons JF, and Wallis NG (2016) Emergence of resistance to tyrosine kinase inhibitors in non-small-cell lung cancer can be delayed by an upfront combination with the HSP90 inhibitor onalespib. *Br J Cancer* 115:1069-1077. doi: 10.1038/bjc.2016.294.

JPET #241661

Farmer H, McCabe N, Lord CJ, Tutt ANJ, Johnson DA, Richardson TB, Santarosa M, Dillon KJ, Hickson I, Knights C, Martin NMB, Jackson SP, Smith GCM, and Ashworth A (2005) Targeting the DNA repair defect in BRCA mutant cells as a therapeutic strategy. *Nature* 434: 917-921.

Ferguson PJ, Brisson AR, Koropatnick J, and Vincent MD (2009) Enhancement of cytotoxicity of natural product drugs against multidrug resistant variant cell lines of human head and neck squamous cell carcinoma and breast carcinoma by tesmilifene. *Cancer Lett* 274: 279-289.

Ferguson PJ, Rytelewski M, Vincent MD, Figueredo R, and Koropatnick J (2013) Sensitization of human tumor cells to chemotherapy drugs by antisense downregulation of BRCA2 and thymidylate synthase (TS): Induction of synthetic lethality by targeting DNA repair. *Proc Amer Assoc Cancer Res* 54: Abst. 3314.

Ferguson PJ, Rytelewski M, Vincent MD, and Koropatnick J (2016) Sensitization of human tumor cells to chemotherapy drugs by antisense downregulation of RAD51: Targeting DNA repair to induce synthetic lethality. *Proc Amer Assoc Cancer Res* 57: Abst. 3718.

Godin SK, Sullivan MR, and Bernstein KA (2016) Novel insights into RAD51 activity and regulation during homologous recombination and DNA replication. *Biochem Cell Biol* 94: 407-418. doi: 10.1139/bcb-2016-0012

Huang F, Mazina OM, Zentner IJ, Cocklin S, and Mazin AV (2012) Inhibition of homologous recombination in human cells by targeting RAD51 recombinase. *J Med Chem* 55: 3011-3020. dx.doi.org/10.1021/jm201173g

JPET #241661

Jhaveri K, Ochiana SO, Dunphy MP, Gerecitano JF, Corben AD, Peter RI, Janjigian YY, Gomes-DaGama EM, Koren J, III, Modi S, and Chiosis G (2014) Heat shock protein 90 inhibitors in the treatment of cancer: current status and future directions. *Expert Opin Investig Drugs* 23: 611-628. doi: 10.1517/13543784.2014.902442.

Jiang J, Lu Y, Li Z, Li L, Niu D, Xu W, Liu J, Fu L, Zhou Z, Gu Y, and Xia F (2017) Ganetespib overcomes resistance to PARP inhibitors in breast cancer by targeting core proteins in the DNA repair machinery. *Invest New Drugs* doi: 10.1007/s10637-016-0424-x. (epub ahead of print)

Ko JC, Chen HJ, Huang YC, Tseng SC, Weng SH, Wo TY, Huang YJ, Chiu HC, Tsai MS, Chiou RY, and Lin YW (2012) HSP90 inhibition induces cytotoxicity via down-regulation of Rad51 expression and DNA repair capacity in non-small cell lung cancer cells. *Regul Toxicol Pharmacol* 64:415-424. doi: 10.1016/j.yrtph.2012.10.003.

Ko JC, Chen JC, Wang TJ, Zheng HY, Chen WC, Chang PY, and Lin YW (2016) Astaxanthin down-regulates Rad51 expression via inactivation of AKT kinase to enhance mitomycin C-induced cytotoxicity in human non-small cell lung cancer cells. *Biochem Pharmacol* 105: 91-100. doi: 10.1016/j.bcp.2016.02.016.

Lapointe H, Lampe H, and Banerjee D (1992) Head and neck squamous cell carcinoma cell line-induced suppression of in vitro lymphocyte proliferative responses. *Otolaryngol Head Neck Surg* 106:149-158.

Lee W-H, Chen P-L, and Zhu J (2009) Compositions and methods for disruption of BRCA2-RAD51 interaction. United States Patent Application Publication Number US

2009/0221634 A1.

Lv W, Budke B, Pawlowski M, Connell PP, and Kozikowski AP (2016) Development of small molecules that specifically inhibit the D-loop activity of RAD51. *J Med Chem* 59: 4511-4525.

Noguchi M, Yu D, Hirayama R, Ninomiya Y, Sekine E, Kubota N, Ando K, and Okayasu R (2006). Inhibition of homologous recombination repair in irradiated tumor cells pretreated with Hsp90 inhibitor 17-allylamino-17-demethoxygeldanamycin. *Biochem Biophys Res Commun* 351: 658-663.

Radujkovic A, Schad M, Topaly J, Veldwijk MR, Laufs S, Schultheis BS, Jauch A, Melo JV, Fruehauf S, and Zeller WJ (2005) Synergistic activity of imatinib and 17-AAG in imatinib-resistant CML cells overexpressing BCR-ABL - Inhibition of P-glycoprotein function by 17-AAG. *Leukemia* 19: 1198-1206.

Rytelewski M, Ferguson PJ, Maleki Vareki S, Figueredo R, Vincent M, and Koropatnick J (2013) Inhibition of BRCA2 and thymidylate synthase creates multidrug sensitive tumor cells via the induction of combined “complementary lethality”. *Molec Ther - Nucl Acids* 2, e78: 1-10; doi:10.1038/mtna.2013.7.

Rytelewski M, Maleki Vareki S, Mangala LS, Romanow L, Jiang D, Pradeep S, Rodriguez-Aguayo C, Lopez-Berestein G, Figueredo R, Ferguson PJ, Vincent M, Sood AK, and Koropatnick JD (2016) Reciprocal positive selection for weakness - preventing olaparib resistance by inhibiting BRCA2. *Oncotarget* 7: 20825-20839. doi: 10.18632/oncotarget.7883

Segawa T, Fujii Y, Tanaka A, Bando S, Okayasu R, Ohnishi K, and Kubota N (2014)

JPET #241661

Radiosensitization of human lung cancer cells by the novel purine-scaffold Hsp90 inhibitor, PU-H71. *Int J Mol Med* 33: 559-564. doi: 10.3892/ijmm.2013.1594.

Slovak ML, Ho JP, Bhardwaj G, Kurz EU, Deeley RG, and Cole SP (1993) Localization of a novel multidrug resistance-associated gene in the HT1080/DR4 and H69AR human tumor cell lines. *Cancer Res* 53: 3221-3225.

Slupianek A, Schmutte C, Tomblin G, Nieborowska-Skorska M, Hoser G, Nowicki MO, Pierce AJ, Fishel R, and Skorski T (2001) BCR/ABL regulates mammalian rec a homologs, resulting in drug resistance. *Mol Cell* 8: 795-806.

Smyth T, Van Looy T, Curry JE, Rodriguez-Lopez AM, Wozniak A, Zhu M, Donsky R, Morgan JG, Mayeda M, Fletcher JA, Schöffski P, Lyons J, Thompson NT, and Wallis NG (2012) The HSP90 inhibitor, AT13387, is effective against imatinib-sensitive and -resistant gastrointestinal stromal tumor models. *Mol Cancer Ther* 11:1799-1808. doi: 10.1158/1535-7163.MCT-11-1046

Suhane T, Laskar S, Advani S, Roy N, Varunan S, Bhattacharyya D, Bhattacharyya S, and Bhattacharyya MK (2015) Both the charged linker region and ATPase domain of Hsp90 are essential for Rad51-dependent DNA repair. *Eukaryot Cell* 14: 64-77. doi: 10.1128/EC.00159-14.

Wiegman AP, Miranda M, Wen SW, Al-Ejeh F, and Möller A (2016) RAD51 inhibition in triple negative breast cancer cells is challenged by compensatory survival signaling and requires rational combination therapy. *Oncotarget* 7: 60087-60100. doi: 10.18632/oncotarget.11065.

Zhong X, Luo G, Zhou X, Luo W, Wu X, Zhong R, Wang Y, Xu F, and Wang J (2016)

JPET #241661

Rad51 in regulating the radiosensitivity of non-small cell lung cancer with different epidermal growth factor receptor mutation status. *Thorac Cancer* 7: 50-60. doi: 10.1111/1759-7714.12274.

Zhu J, Zhou L, Wu G, Konig H, Lin X, Li G, Qiu XL, Chen CF, Hu CM, Goldblatt E, Bhatia R, Chamberlin AR, Chen PL, and Lee WH (2013) A novel small molecule RAD51 inactivator overcomes imatinib-resistance in chronic myeloid leukaemia. *EMBO Mol Med* 5: 353-365. doi:10.1002/emmm.201201760

Footnotes

This work was supported by a grant from the Medical Oncology Research Fund, London Regional Cancer Program, London Health Sciences Centre, London, Canada.

¹ American Type Culture Collection, www.atcc.org

Figure Legends

Figure 1. IC_{50} values for IBR2, imatinib, and regorafenib tested against a range of cell lines *in vitro*. Cells were grown in 96-well plates, and exposed to a range of concentrations of drug. Relative cell density was determined by a viability assay (alamarBlue© or neutral red). The concentration of drug that inhibited proliferation by 50% was interpolated from plotted data. Bars represent means of between 3 and 29 determinations (except n=1 for: K562, Panel 1; H1650 and H1975, Panels B and C); *error bars*, SD.

Figure 2. Quantitation of enhancement of cytotoxicity of imatinib by IBR2. Panel A - A representative experiment demonstrating the ability of IBR2 to enhance the antiproliferative activity of imatinib against AGS gastric carcinoma cell line. Cells were grown in 96-well plates, and treated with simultaneous exposure to IBR2 and the drugs at the concentrations indicated. The relative cell density was determined after 4 days by viability staining. The relative density of cells treated with both agents was normalized to the density observed for the respectively treated IBR2 control. The concentration of drug that inhibited proliferation by 50% was interpolated from plotted data. The change in the IC_{50} value caused by the presence of IBR2 was determined as a percent of the IC_{50} of imatinib in the absence of IBR2. Therefore, enhancement of cytotoxicity (synergistic drug interaction), exemplified by a decrease in the IC_{50} value, manifests as a negative value. These values were determined over a range of concentrations of IBR2 in a variety of cell lines, and compiled to create Panels B - D: Enhancement of imatinib cytotoxicity by IBR2 in NSCLC cell lines (B), gastric and colon carcinoma cell lines (C), and CML, HNSCC and kidney cell lines (D).

JPET #241661

Figure 3. Enhancement of cytotoxicity of regorafenib by IBR2. Cells were grown in 96-well plates, and treated with simultaneous exposure to the drugs at the concentrations indicated. The relative cell density was determined after 4 days by viability staining. The relative density of cells treated with both agents was normalized to the density observed for the respectively treated IBR2 control. The concentration of drug that inhibited proliferation by 50% was interpolated from plotted data. The change in the IC_{50} value caused by the presence of IBR2 was determined as a percent of the IC_{50} of regorafenib in the absence of IBR2. Negative values indicate synergy. These values were determined over a range of concentrations of IBR2 in a variety of cell lines, and compiled to create Panels A - C: Enhancement of regorafenib cytotoxicity by IBR2 in NSCLC and SCLC cell lines (A), gastric and colon carcinoma cell lines (B), and leukemic and breast cancer cell lines (C).

Figure 4. Enhancement of inhibitors of EGFR in NSCLC cell lines by IBR2. Cells were grown in 96-well plates, and treated with simultaneous exposure to IBR2 and the drugs at the concentrations indicated. The relative cell density was determined after 4 days by viability staining. The relative density of cells treated with both agents was normalized to the density observed for the respectively treated IBR2 control. The concentration of drug that inhibited proliferation by 50% was interpolated from plotted data. The change in the IC_{50} value caused by the presence of IBR2 was determined as a percent of the IC_{50} of EGFR inhibitor in the absence of IBR2. Negative values indicate synergy. These values were determined over a range of concentrations of IBR2 in combination with gefitinib (Panel A), erlotinib (B), afatanib (C), and osimertinib (D). The IC_{50} values for gefitinib, erlotinib, afatanib and osimertinib, respectively,

JPET #241661

for A549b were: 14.3 ± 2.9 (6), 7.2 ± 1.2 (6), 4.15 (1), and 6.16 (1); for H1650: 11.2 ± 1.4 (3), 18.7 ± 3.7 (3), 1.83 ± 0.22 (3), and 3.53 ± 0.11 (3); for H1975: 13.8 ± 1.0 (3); 9.7 ± 0.3 (3); 0.38 ± 0.08 (3); 0.034 ± 0.013 (3); for HEK293, 8.88 ± 0.45 (3) for gefitinib, 2.33 ± 1.14 (3) for osimertinib.

Figure 5. Comparison of enhancement of imatinib cytotoxicity caused by IBR2, verapamil, or B02 (enhancers). Cells were grown in 96-well plates, and treated with simultaneous exposure to the drugs at the concentrations indicated. The relative cell density was determined after 4 days by viability staining. The relative density of cells treated with both agents was normalized to the density observed for the respectively treated enhancer control. The concentration of imatinib that inhibited proliferation by 50% was interpolated from plotted data, as indicated in Figure 1. The change in the IC_{50} value caused by the presence of enhancer was determined as a percent of the IC_{50} of imatinib in the absence of enhancer. Negative values indicate synergy. These values were determined over a range of concentrations of enhancer plus imatinib against carcinoma cell lines A549b (Panel A), HT-29 (B), HN-5a (C), and HN-5a/V15e (D). Points are means of 3 to 6 determinations [with error bars (SD)] or are from single experiments (no error bars); *, $P < 0.05$. The IC_{50} values for IBR2 and imatinib for these cell lines are indicated in Figure 1. The IC_{50} values for verapamil for the respective cell lines (above) are: 88.7 ± 0.9 (3), 17.6 ± 0.7 (5), 89.4 ± 7.7 (3), and 99.2 ± 1.2 (2). The IC_{50} values for B02 for the respective cell lines are: 11.8 ± 2.1 (6), 10.4 ± 2.1 (8), 12.2 ± 0.9 (4), and 15.0 ± 5.4 (3).

Figure 6. Comparison of enhancement of vincristine cytotoxicity caused by IBR2, verapamil, or B02 (enhancers). Cells were grown in 96-well plates, and treated with simultaneous exposure to

JPET #241661

the drugs at the concentrations indicated. The relative cell density was determined after 4 days by viability staining. The relative density of cells treated with both agents was normalized to the density observed for the respectively treated enhancer control. The concentration of vincristine that inhibited proliferation by 50% was interpolated from plotted data. The change in the IC₅₀ value caused by the presence of enhancer was determined as a percent of the IC₅₀ of vincristine in the absence of enhancer. Negative values indicate synergy. These values were determined over a range of concentrations of enhancer plus vincristine against carcinoma cell lines A549b (Panel A), HT-29 (B), HN-5a (C), and HN-5a/V15e (D). Points are means of 2 to 6 determinations [with error bars (SD)] or are from single experiments (no error bars). The IC₅₀ values for vincristine for each of the cell lines are, respectively: 4.34 ± 0.45 (n=9); 3.61 ± 0.56 (15); 4.36 ± 0.92 (6); 11.7 ± 3.3 (12). The IC₅₀ values for IBR2 for these cell lines are indicated in Figure 1. The IC₅₀ values for verapamil and B02 are listed in the legend for Figure 5.

Figure 7. Comparison of effect of RAD51 antisense molecule and RAD51 inhibitor IBR2 on the cytotoxicity of olaparib and other anticancer drugs. Panels A, C and D - Cells were cultured in 25-cm² flasks, and exposed to siRNA as described in “Materials and Methods”, for 4 h, followed by addition of one volume of medium. After a further 20 h, the medium was changed and the drug indicated was added to the final desired concentration. The proliferation of cells in the presence of the indicated concentration of siRNA, as a percent of the scrambled siRNA control, in Panel A was, for A549b, 85.3 ± 11.0 % (n=9), and for HT-29, 70.2 ± 11.9 (7). In Panel C and D, proliferation was, for A549b, 51.8 ± 12.7 % (8), and for DU145, 62.4 ± 11.6 % (9). Panel B - A549b cells were grown in 96-well plates, and treated with simultaneous exposure to IBR2 and

JPET #241661

olaparib at the concentrations indicated. The relative cell density was determined after 4 days by viability staining. The relative density of cells treated with both agents was normalized to the density observed for the respectively treated IBR2 control. The concentration of drug that inhibited proliferation by 50% was interpolated from plotted data. The change in the IC₅₀ value caused by anti-RAD51 antisense or the presence of IBR2 was determined as a percent of the IC₅₀ of drug in the absence of co-treatment. Negative values indicate synergy, whereas positive values indicate antagonism. *, $P < 0.05$. Imat, imatinib; Gefit, gefitinib; Osim, osimertinib; VCR, vincristine.

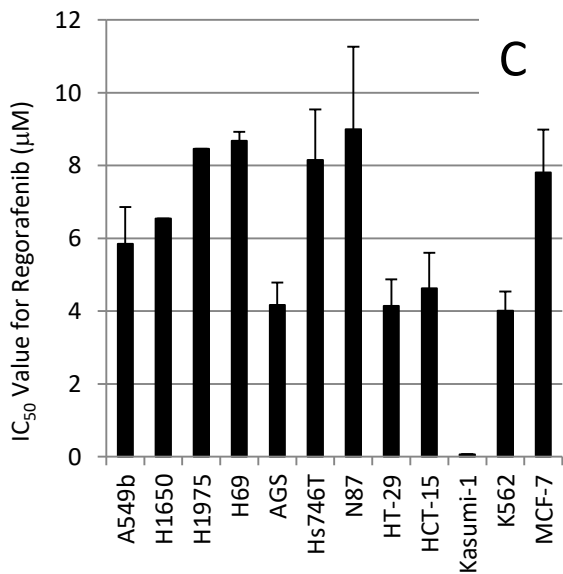
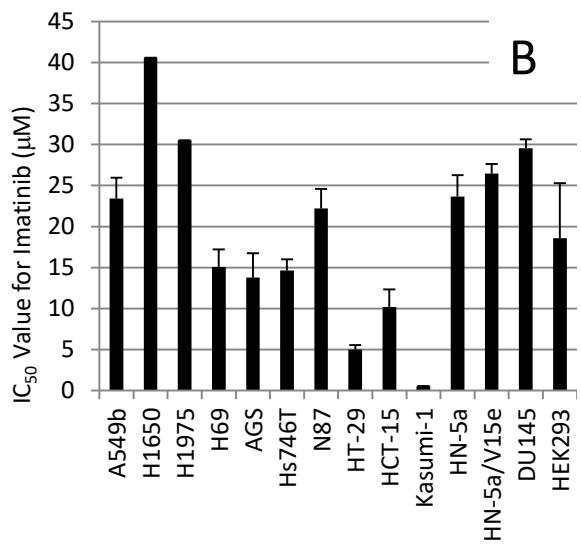
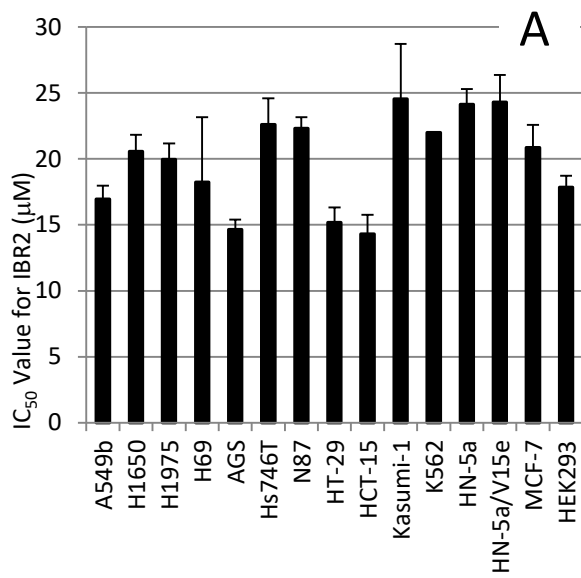


Figure 1

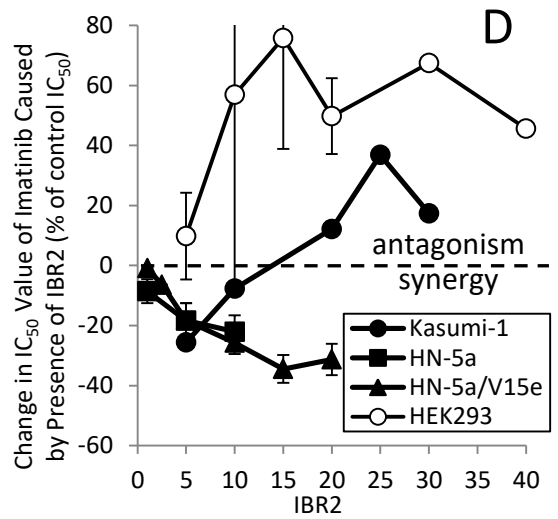
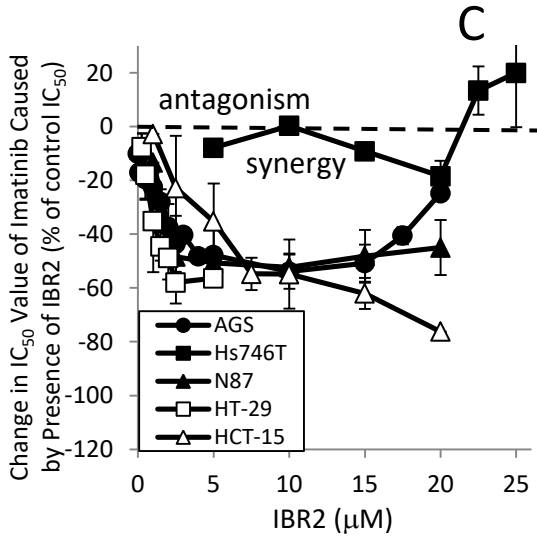
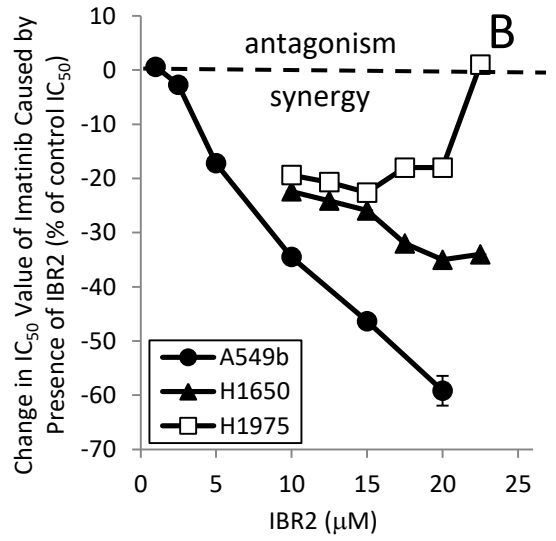
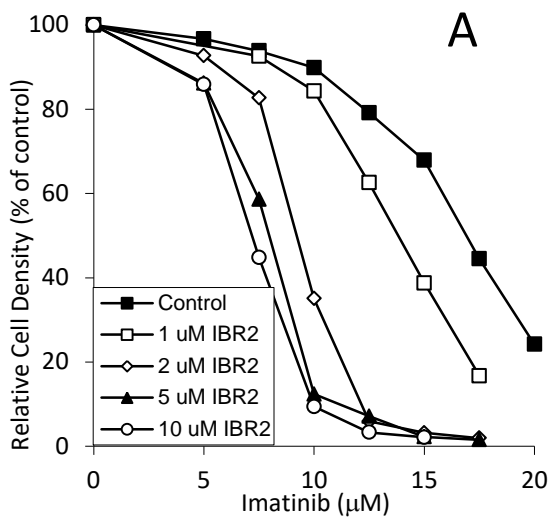


Figure 2

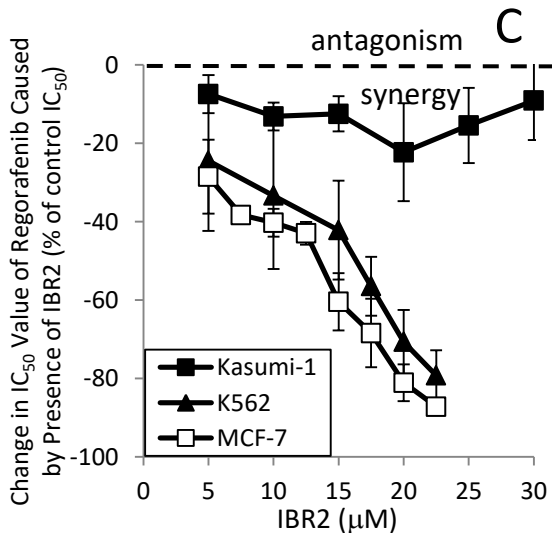
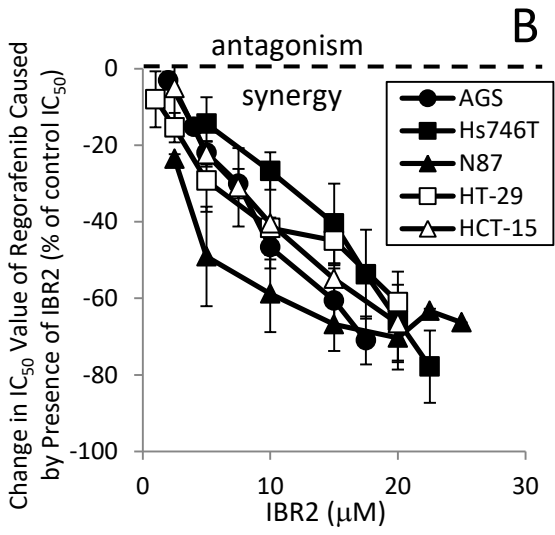
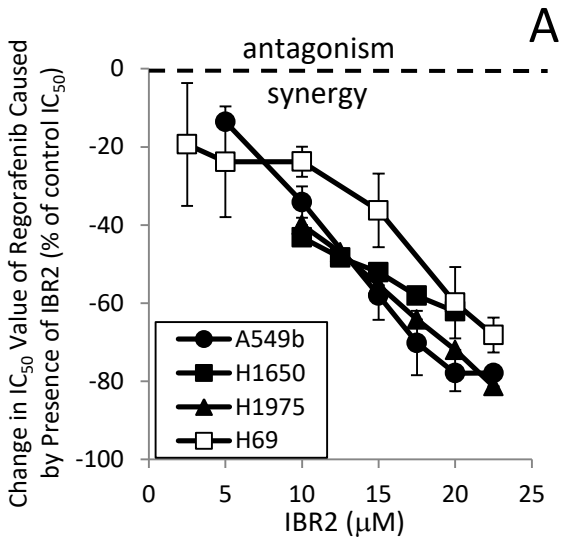


Figure 3

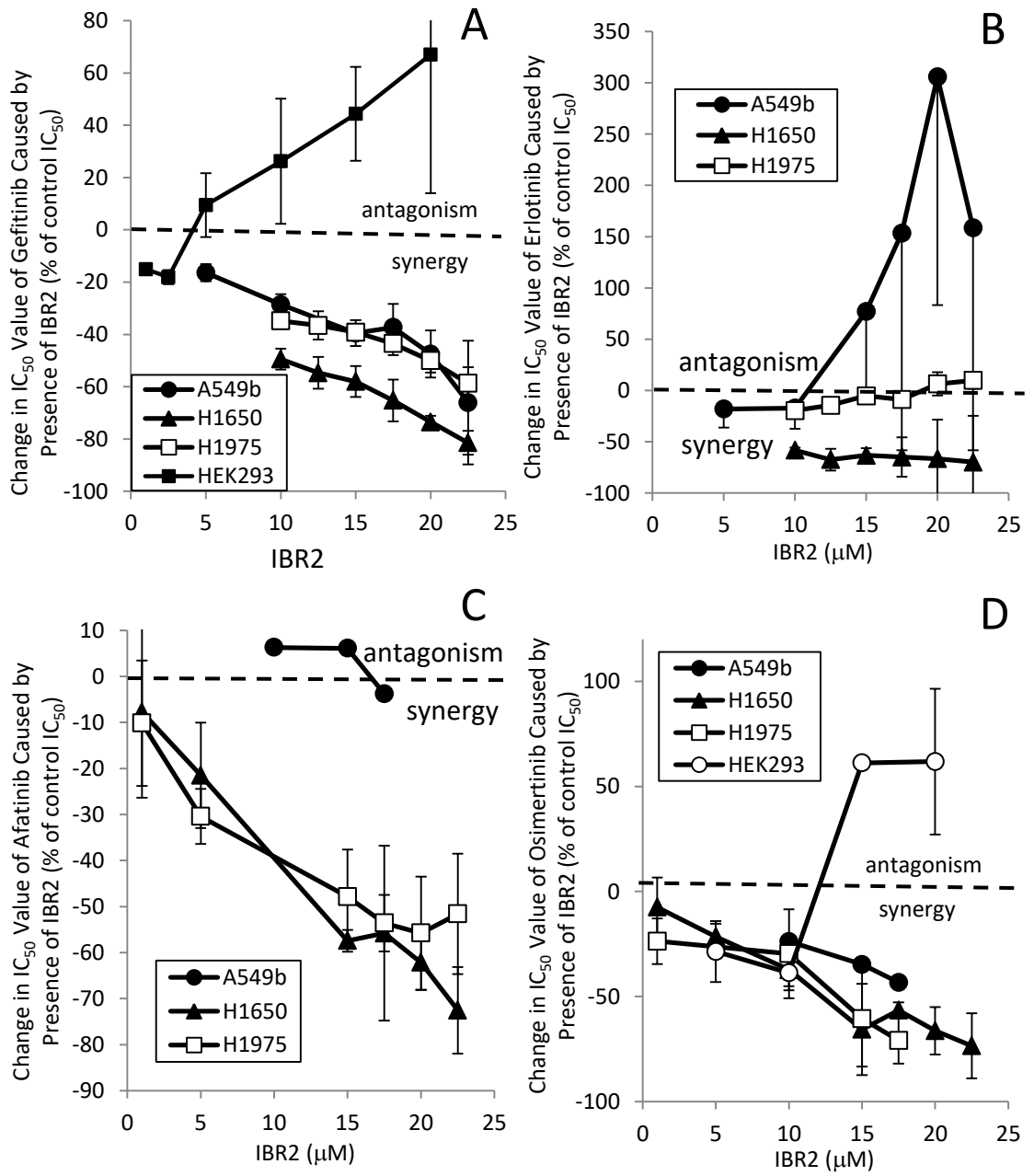


Figure 4

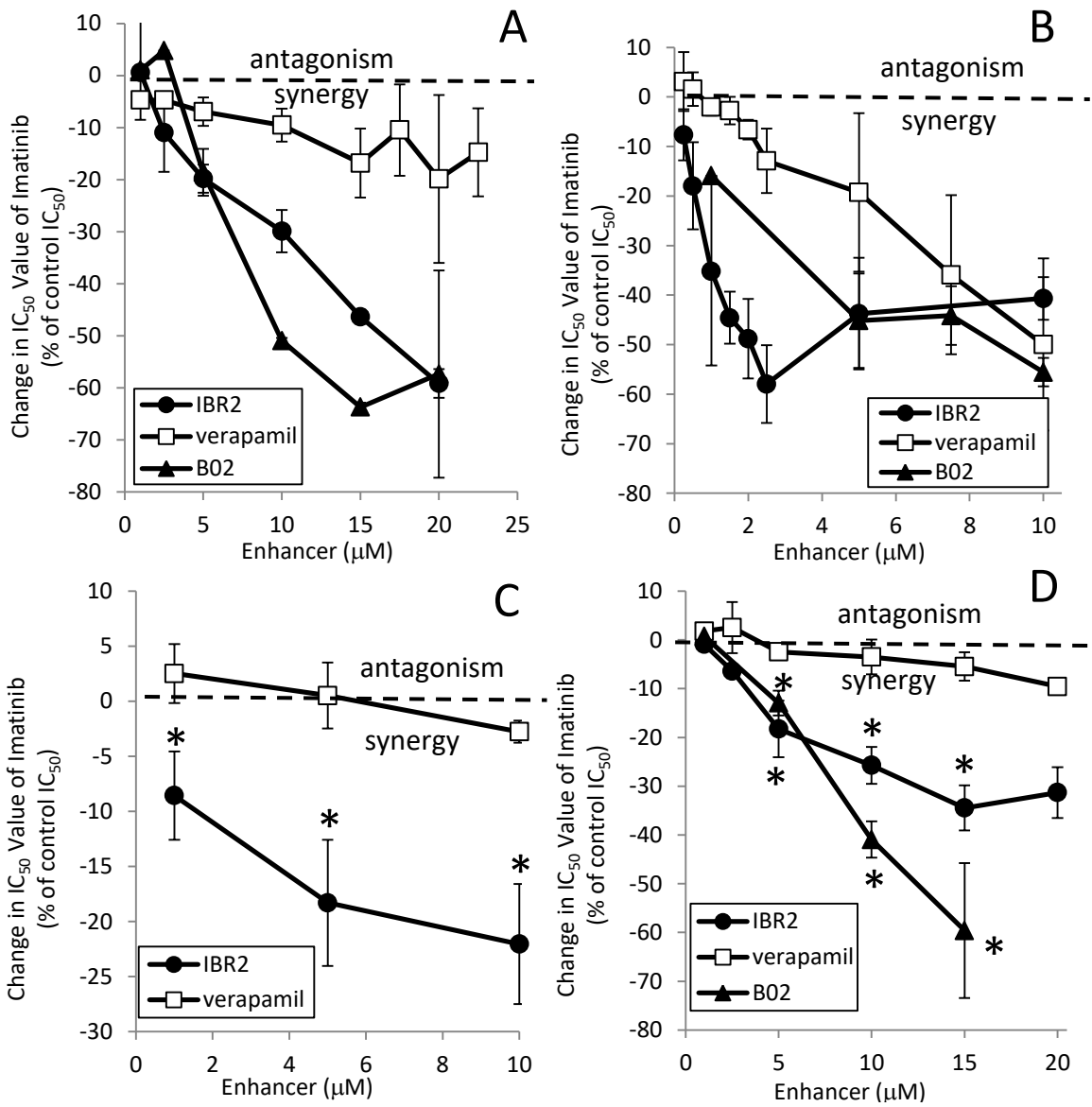


Figure 5

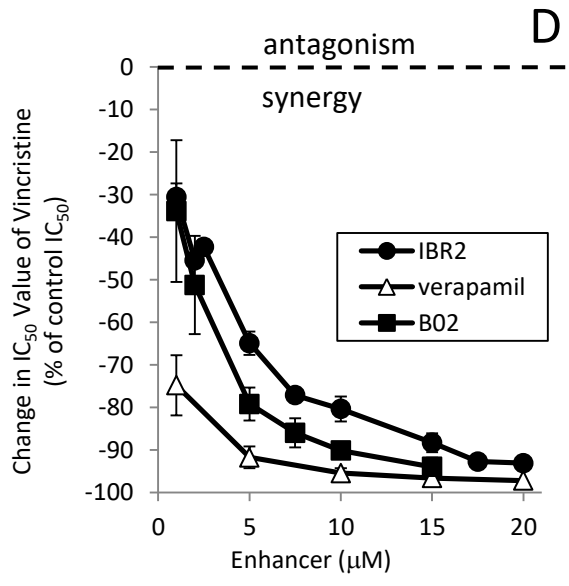
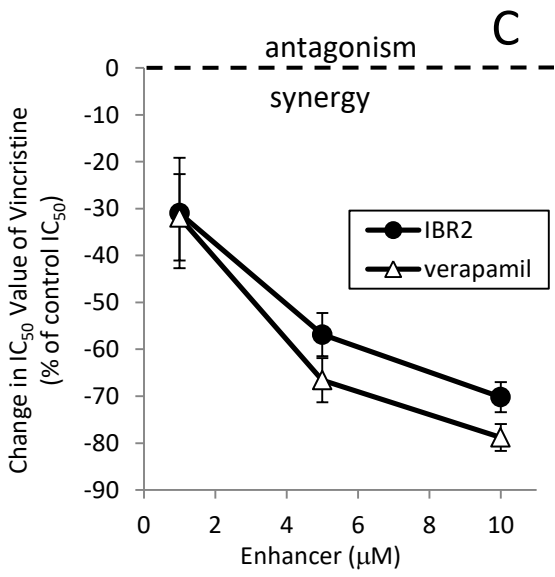
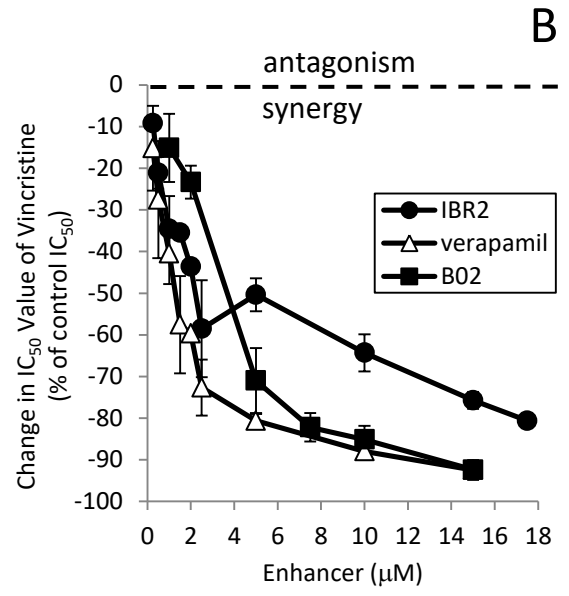
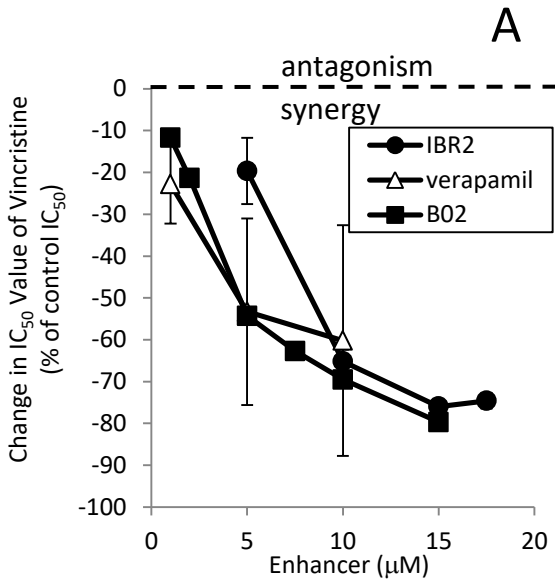
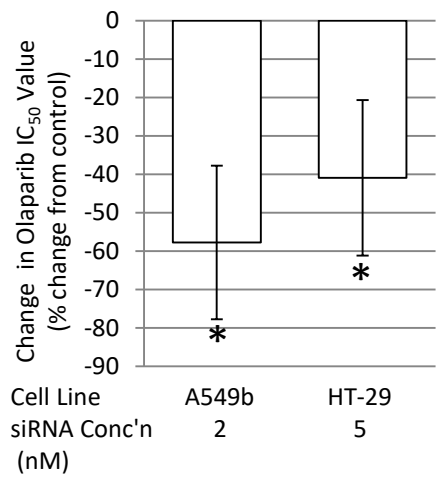
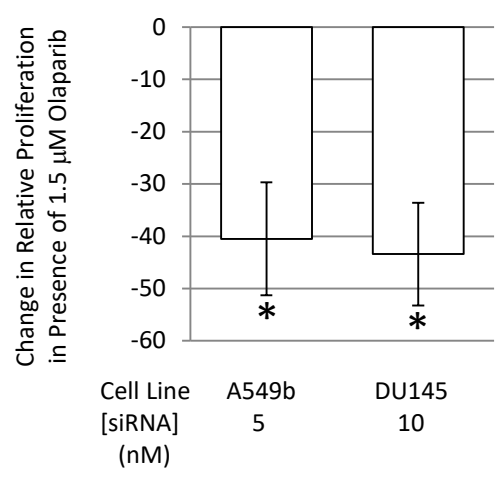


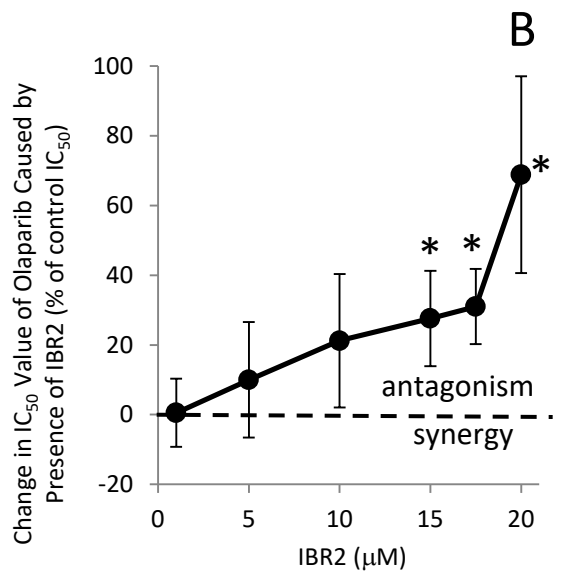
Figure 6



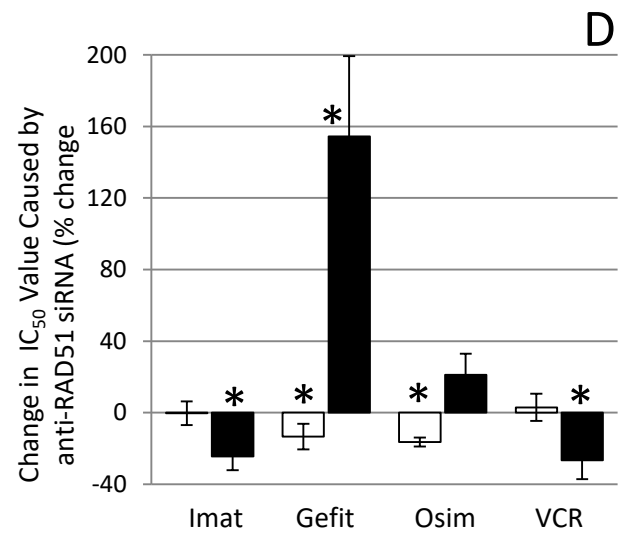
A



C



B



D

Figure 7